ELSEVIER

Engineering Analysis with Boundary Elements 27 (2003) 655–670

ENGINEERING ANALYSIS *with* BOUNDARY ELEMENTS

www.elsevier.com/locate/enganabound

Study on the true and spurious eigensolutions of two-dimensional cavities using the dual multiple reciprocity method

J.T. Chen*, S.R. Kuo, I.L. Chung, C.X. Huang

Department of Harbor and River Engineering, National Taiwan Ocean University, Keelung, Taiwan, ROC

Received 23 October 2001; revised 8 May 2002; accepted 15 May 2002

Abstract

In this paper, true and spurious eigensolutions for a circular cavity using the dual multiple reciprocity method (MRM) are analytically derived and numerically verified by the developed program. The roots of spurious eigenequation are found analytically by using symbolic manipulation software. A more efficient method is proposed by choosing a fewer number of equations from the dual MRM instead of all of the equations in the dual MRM. Numerical experiments are performed by using dual MRM program for comparison purposes. A circular cavity of radius 1 m with Neumann boundary conditions is considered, and the results match very well between the theoretical prediction and the numerical experiments for the first four true eigenvalues and the first two spurious eigenvalues. Also, a noncircular case of square cavity is numerically implemented. The true eigensolutions can be easily solved by the dual MRM program in conjunction with the singular value decomposition technique. At the same time, the boundary modes and the multiplicities of the true eigenvalues can also be determined.
© 2003 Elsevier Ltd. All rights reserved.

Keywords: Eigensolution; Circular cavity; Helmholtz equation; Dual series model; Spurious eigenvalues; SVD and dual MRM

1. Introduction

The multiple reciprocity method (MRM) has been widely used to transform domain integrals into boundary integrals for the Helmholtz and the Poisson equations [1]. For the Helmholtz equation, one advantage of using MRM is that only real-variable computation is considered instead of complex variable computation as used in the complex-valued boundary element method. It is found that MRM is no more than the real part of a complex-valued formulation [2–5]. A simplified method using only a real-part or imaginary-part kernel was also presented by De Mey [6]. However, one drawback of MRM has been found to be the occurrence of spurious eigenvalues [8]. To deal with this problem, the framework of dual MRM was constructed so as to filter out spurious eigenvalues. A detailed review article on the dual formulation, including 250 references, by Chen and Hong [12,13] can be referred to. Spurious eigenvalues occur in the MRM due to the loss of the imaginary part, which was investigated in Ref. [15]. Also, the relation between MRM and complex-valued BEM was discussed in a keynote lecture by Chen [3]. The occurrence of spurious eigensolutions can be avoided in three ways: one is the complex-valued formulation [16], another is the dual approach [8,17] and the other is the domain-partition method [7]. By employing the dual MRM, spurious eigenvalues can be filtered out by checking the residual between the singular and hypersingular equations in the dual MRM. A two-dimensional case was studied in Ref. [17]. However, the boundary modes (including true and spurious cases) should be determined in advance before finding the residue. Finding a more efficient method to distinguish whether an eigenvalue is true or not is not trivial. Therefore, the SVD technique was employed to filter out spurious eigenvalues for two-dimensional cavities [9–11] and one-dimensional problems [18,19] with greater efficiency than using the residue method presented in Ref. [17]. After finding the true eigenvalues, determining their multiplicities is our concern. Furthermore, predicting spurious solutions analytically is the main focus of this research. In Ref. [20], sensitivity and failure in determining boundary modes and interior modes were discussed for the case where the normalized value is set to one at the boundary point with exact solution of zero or near zero. To avoid this problem, the SVD technique is also employed here to determine the boundary modes even

* Corresponding author. Tel.: +886-2-2462-2192; fax: +886-2-2462-0724.

0955-7997/03/$ - see front matter © 2003 Elsevier Ltd. All rights reserved.
doi:10.1016/S0955-7997(03)00019-5

though a double root is available. This technique can be applied to not only a circular-boundary problem, but also general boundary problem. In the dual MRM [10] or real-part BEM [9,11], all the equations in the dual formulation are combined to filter out the spurious solutions since the rank deficiency can be improved. It is found that only rank one or two deficiency is present in the real UT or LM formulation [9–11], a sufficient number of independent equations from LM or UT formulation is required. Based on the concept of CHIEF method, the sufficient number of independent equations should be provided to improve the rank deficiency. Therefore, a more efficient method by choosing a fewer number of equations from dual formulation than all of them in the dual MRM [9–11] is proposed.

In this paper, we employ dual MRM to solve for the eigensolutions of a circular cavity analytically and numerically. For circular and noncircular cases, we select sufficient number of equations from the dual MRM to filter out spurious solutions more efficiently. After assembling the sufficient equations in the dual MRM, the singular value decomposition (SVD) technique presented in Ref. [19] is extended to filter out spurious eigenvalues for two-dimensional cavities with greater efficiency than can be obtained using the residue method described in Ref. [17]. The spurious eigensolutions (including eigenvalues and eigenfunctions) are investigated analytically and found numerically. Also, the boundary modes and the multiplicities of the true eigenvalues are determined using the same method. These two roles of the SVD technique in the dual MRM are both examined. One example of a circular cavity subject to the Neumann boundary condition is employed to check the validity of the analytical method. A noncircular case of square cavity is also considered numerically. Finally, the solutions are compared with the exact solutions to check the validity of the present formulation.

2. Dual integral formulation of MRM for a two-dimensional acoustic cavity

The governing equation for an acoustic cavity is the Helmholtz equation:

$$(\nabla^2 + k^2)u(x_1, x_2) = 0, \qquad (x_1, x_2) \in D,$$

where ∇^2 is the Laplacian operator, D is the domain of the cavity and k is the wave number, which is the frequency over the speed of sound. The boundary conditions can be either of the Neumann or of the Dirichlet type.

Based on the dual multiple reciprocity method (MRM) [1,10,17], the dual MRM equations for the boundary points are

$$u(x) = \text{CPV}\int_B T(s,x)u(s)\mathrm{d}B(s) - \text{RPV}\int_B U(s,x)t(s)\mathrm{d}B(s), \qquad x \in B, \tag{1}$$

$$t(x) = \text{HPV}\int_B M(s,x)u(s)\mathrm{d}B(s) - \text{CPV}\int_B L(s,x)t(s)\mathrm{d}B(s), \qquad x \in B, \tag{2}$$

where CPV, RPV and HPV denote the Cauchy principal value, the Riemann principal value and the Hadamard principal value, $t(s) = (\partial u(s)/\partial n_s)$, B denotes the boundary enclosing D and the four kernels are series forms which can be found in Ref. [17].

3. Dual MRM for an acoustic cavity using the constant element scheme

By discretizing the boundary B into boundary elements in Eqs. (1) and (2), we obtain the dual algebraic system as follows

$$\pi\{u\} = [T]\{u\} - [U]\{t\}, \tag{3}$$

$$\pi\{t\} = [M]\{u\} - [L]\{t\}, \tag{4}$$

where the $[U]$, $[T]$, $[L]$ and $[M]$ matrices are the corresponding influence coefficient matrices resulting from the 10-terms of the U, T, L and M series kernels, respectively. The detailed derivation for the singular and hypersingular integrals can be found in Refs. [10,17]. Eqs. (3) and (4) can be rewritten as

$$[\bar{T}]\{u\} = [U]\{t\}, \tag{5}$$

$$[M]\{u\} = [\bar{L}]\{t\}, \tag{6}$$

where $[\bar{T}] = [T] - \pi[I]$ and $[\bar{L}] = [L] + \pi[I]$. The computational issues for the dual MRM can be found in Refs. [10,17]. The developed DUALMRM program was utilized here in the numerical study.

4. Detection of spurious eigenvalues and determination of the multiplicities of the true eigenvalues using the singular value decomposition technique for dual MRM

According to Eqs. (5) and (6), we can obtain the eigenvalues independently for the problem without degenerate boundaries. However, spurious roots are imbedded if the UT equation (5) or LM equation (6) is used alone. As mentioned by Kamiya et al. [2], the equation derived using MRM is no more than the real part of the complex-valued formulation. The loss of the imaginary part in MRM results in spurious roots. Yeih et al. [15] extended the general proof for any dimensional problems and demonstrated it using a one-dimensional case. The imaginary part in the complex-valued formulation is not present in MRM, and the number of constraints for the eigenequation is insufficient, which causes the solution space to become larger. These findings can explain why spurious roots occur using MRM when

either Eq. (5) or Eq. (6) only is employed; i.e. the mechanism of the spurious roots can be understood in this way. The technique used to filter out spurious eigenvalues in Refs. [10,17] is summarized as follows.

Since only the real part is of concern in MRM, one approach to obtaining enough constraints for the eigenequation instead of the imaginary part of the complex-valued formulation is to perform differentiation with respect to the conventional MRM. This method results in the hypersingular formulation for MRM. For the sake of simplicity, we will deal with the Neumann problem. Therefore, Eqs. (5) and (6) reduce to

$$[\bar{T}(k)]_{N\times N}\{u\}_{N\times 1} = \{0\}, \tag{7}$$

$$[M(k)]_{N\times N}\{u\}_{N\times 1} = \{0\}, \tag{8}$$

where N is the number of boundary elements. In Ref. [17], an approach to detecting spurious roots is to use the criterion of the residue to satisfy Eq. (5) (or Eq. (6)) when substituting the boundary modes obtained from Eq. (6) (or Eq. (5)) for the characteristic wave number, k. The spurious modes obtained from Eq. (5) will not satisfy Eq. (6). The proof will be elaborated on later in Eqs. (52)–(55). This conclusion also matches well with the results of fictitious frequency in exterior acoustics. Burton and Miller proposed a combined approach of UT and LM equations since their fictitious poles are not the same [14]. Also, the spurious modes obtained from Eq. (6) will not satisfy Eq. (5) in controversa. Therefore, two residual norms can be defined as follows [17]

$$\epsilon_T = [\bar{T}(k_M)]\{u_M\}, \tag{9}$$

where $\{u_M\}$ is the boundary mode which satisfies $[M(k_M)]\{u_M\} = \{0\}$; and

$$\epsilon_M = [M(k_T)]\{u_T\}, \tag{10}$$

where $\{u_T\}$ is the boundary mode which satisfies $[\bar{T}(k_T)]\{u_T\} = 0$; ϵ_T and ϵ_M are the residue norms induced by Eqs. (9) and (10), respectively; and k_M and k_T are the possible (true or spurious) eigenvalues obtained by Eqs. (7) and (8), respectively. By setting an appropriate value of the threshold, we can determine whether the root is true or spurious. To double check, the acoustic modes can be examined based on the distribution of nodal lines and orthogonal properties after the possible true eigenvalues are determined [17].

It is noted here that the residue method needs to find the spurious boundary modes first from one equation (either the UT or LM equation) in the stage in which we directly search for the eigenvalue, and then substitute it into another eigenequation (either the LM or UT equation) to check the residuals. Now, we will present a more efficient way to filter out spurious eigenvalues which can avoid the need to determine the spurious boundary mode in advance.

To filter out spurious eigenvalues using the SVD technique, we can merge the two matrices in Eqs. (7) and (8) together to obtain an overdeterminate system as

$$[C(k)]_{2N\times N}\{u\}_{N\times 1} = \{0\}, \tag{11}$$

where the $[C(k)]$ matrix is the augmented matrix, by combining the $[\bar{T}]$ and $[M]$ matrices as shown below [10]

$$[C(k)]_{(2N)\times N} = \begin{bmatrix} M_{N\times N}(k) \\ k\bar{T}_{N\times N}(k) \end{bmatrix} \tag{12}$$

for the Neuman problem,

where the k term in Eq. (12) is added to be consistent in dimension. Even though the $[C(k)]$ matrix in Eq. (12) may have dependent rows resulting from the degenerate boundary, the SVD technique can still be employed to find all the true eigenvalues since a sufficient number of constraints are imbedded in the overdeterminate matrix, $[C(k)]$. As for the true eigenvalues, the rank of the $[C(k)]$ matrix with dimension $2N \times N$ must at most be $N - 1$ to obtain a nontrivial solution. To filter out the spurious eigenvalues, the rank must be promoted to N to obtain a trivial eigensolution. In the dual MRM [10] or real-part dual BEM [9,11], all the equations are combined together to meet the requirement as shown in Eq. (12). However, it is found that UT MRM [10] or real-part BEM [9,11] results in rank deficiency by one and two for single spurious root and double spurious root, respectively. In this paper, we propose a more efficient method by selecting the appropriate number of equations from dual formulation to filter out the spurious eigensolutions as follows:

$$[C(k)]_{(N+2)\times N} = \begin{bmatrix} M_{N\times N}(k) \\ k\bar{T}_{2\times N}(k) \end{bmatrix}. \tag{13}$$

To find the rank of $[C(k)]$ matrix, the SVD technique can be employed to detect the true eigenvalues by checking whether or not the first minimum singular values, σ_1, are zeros. Since discretization creates errors, very small values for σ_1, but not exactly zeros, will be obtained when k is near the critical wave number. In order to avoid the need to determine the threshold for the zero numerically, a value of σ_1 closer to zero must be obtained using a smaller increment for the critical wave number, k. Such a value is confirmed to be a true eigenvalue.

Since Eq. (11) is overdeterminate, we will consider a linear algebra problem with more equations than unknowns

$$[\mathbf{A}]_{m\times n}\{\mathbf{x}\}_{n\times 1} = \{\mathbf{b}\}_{m\times 1}, \qquad m > n, \tag{14}$$

where m is the number of equations, n is the number of unknowns and $[\mathbf{A}]$ is the leading matrix, which can be decomposed into [21,22]

$$[\mathbf{A}]_{m\times n} = [\mathbf{U}]_{m\times m}[\mathbf{\Sigma}]_{m\times n}[\mathbf{V}]^*_{n\times n}, \tag{15}$$

where $[\mathbf{U}]$ is a left unitary matrix constructed by the left singular vectors $(\mathbf{u}_1, \mathbf{u}_2, \mathbf{u}_3, \ldots, \mathbf{u}_m)$, $[\mathbf{\Sigma}]$ is a diagonal matrix which has singular values $\sigma_1, \sigma_2, \ldots,$ and σ_n allocated in

a diagonal line as

$$[\Sigma] = \begin{bmatrix} \sigma_n & \cdots & 0 \\ \vdots & \ddots & \vdots \\ 0 & \cdots & \sigma_1 \\ \vdots & \ddots & \vdots \\ 0 & \cdots & 0 \end{bmatrix}, \qquad m > n, \tag{16}$$

in which $\sigma_n \geq \sigma_{n-1} \cdots \geq \sigma_1$, and $[\mathbf{V}]^*$ is the complex conjugate transpose of a right unitary matrix constructed by the right singular vectors $(\mathbf{v}_1, \mathbf{v}_2, \mathbf{v}_3, \ldots, \mathbf{v}_m)$. As we can see in Eq. (16), there exist at most n nonzero singular values. This means that we can find at most n linear independent equations in the system of equations. If we have p zero singular values ($0 \leq p \leq n$), this means that the rank of the system of equations is equal to $n - p$. However, the singular value may be very close to zero numerically, resulting in rank deficiency. For a general eigenproblem as shown in this paper, the $[C(k)]$ matrix with dimension $2N \times N$ will theoretically have a rank of $N - 1$ for the true eigenvalue with multiplicity 1 and $\sigma_1 = 0$. For true eigenvalues with multiplicity Q, the rank of $[C(k)]$ will be reduced to $N - Q$, in which $\sigma_1, \sigma_2, \ldots, \sigma_Q$ are zeros theoretically. In another words, the matrix has a nullity of Q. In the case of spurious eigenvalues, the rank for the $[C(k)]$ matrix is N, and the minimum singular value is not zero.

Determining the eigenvalues of the system of equations has now been transformed into finding the values of k which make the rank of the leading coefficient matrix smaller than N. This means that when $m = 2N$, $n = N$ and $\mathbf{b}_{2N\times 1} = \mathbf{0}$, the eigenvalues will make $p \geq 1$, such that the minimum singular values must be zero or very close to zero.

According to the definition for SVD, we have

$$[\mathbf{A}]\mathbf{v}_p = \sigma_p \mathbf{u}_p, \qquad p = 1, 2, 3, \ldots, n. \tag{17}$$

By choosing the qth zero singular value, σ_q, and substituting the qth right eigenvector, $\mathbf{v}_q$, into Eq. (17), we have

$$[\mathbf{A}]\mathbf{v}_q = 0\mathbf{u}_q = \mathbf{0}, \qquad q = 1, 2, 3, \ldots, Q. \tag{18}$$

According to Eq. (18), the nontrivial boundary mode is found to be the column vector, $\mathbf{v}_q$, in the right unitary matrix.

After introducing the SVD method, matrix $[C(k)]$ apparently causes the rank of the leading coefficient matrix to be equal to $N - 1$ for the true eigenvalue with multiplicity 1. The boundary modes can be obtained from the $[\mathbf{V}]$ matrix in Eq. (14) using SVD. Another advantage of using SVD is that it can determine the multiplicities for the true eigenvalues by finding the number of near zeros in the singular values. Two examples a circular cavity and a square cavity with eigenvalues of multiplicity 2 will be considered to demonstrate the use of SVD technique.

To check the validity of the proposed method, one example will be examined analytically in the following section.

5. Analytical derivations for true and spurious eigensolutions

It is well known that MRM is no more than the real part of the complex-valued formulation [2,15]. Therefore, the real part of the complex-valued kernel, $U(s,x)$ [23,24], is

$$\mathrm{Re}\left[-\frac{\pi}{2}\mathrm{i}H_0(kr)\right] = \frac{\pi}{2}Y_0(kr), \tag{19}$$

where H_0 and Y_0 are the Hankel and Bessel functions of zero order, respectively. The imaginary part, $J_0(x)$, in $U(s,x)$ is

$$\mathrm{Im}\left[\frac{-\pi\mathrm{i}}{2}H_0(x)\right] = \frac{-\pi}{2}J_0(x) = \frac{-\pi}{2}\sum_{n=0}^{\infty} p_n x^{2n}, \tag{20}$$

where J_0 is the first kind Bessel function of zero order and p_n is

$$p_n = \frac{(-1)^n}{4^n(n!)^2}. \tag{21}$$

Based on the theory of special functions, we can have

$$\begin{aligned} \frac{\pi}{2}Y_0(x) &= \left[\ln\frac{x}{2} + \gamma\right]J_0(x) + \sum_{n=0}^{\infty} q_n x^{2n} \\ &= \left[\ln\frac{x}{2} + \gamma\right]\sum_{n=0}^{\infty} p_n x^{2n} + \sum_{n=0}^{\infty} q_n x^{2n}, \end{aligned} \tag{22}$$

where γ is an Euler constant and q_n is

$$q_n = \frac{(-1)^{(n+1)}}{4^n(n!)^2}\left(1 + \frac{1}{2} + \frac{1}{3} + \cdots + \frac{1}{n}\right). \tag{23}$$

In the present MRM formulation, the real kernel is

$$\frac{\pi}{2}\bar{Y}(kr) \doteq (\ln r)\sum_{n=0}^{10} p_n (kr)^{2n} + \sum_{n=0}^{9} q_n (kr)^{2n} \tag{24}$$

since 10 terms are adopted in the dual MRM program [17]. As kr approaches zero, we have

$$\frac{\pi}{2}\bar{Y}(kr) = \frac{\pi}{2}Y_0(kr) - \left[\ln\frac{k}{2} + \gamma\right]J_0(kr). \tag{25}$$

By setting $x = (\rho, 0)$ and $s = (R, \theta)$ as shown in Fig. 1(a), we can expand $U(s,x)$ into a degenerate kernel as shown below:

$$\begin{aligned} U(s,x) &= \frac{\pi}{2}\bar{Y}(kr) = \frac{\pi}{2}Y_0(kr) - \left[\ln\frac{k}{2} + \gamma\right]J_0(kr) \\ &= \frac{\pi}{2}\sum_{n=-\infty}^{\infty} Y_n(kR)J_n(k\rho)\cos n\theta - \left[\ln\frac{k}{2} + \gamma\right] \\ &\quad \times \sum_{n=-\infty}^{\infty} J_n(kR)J_n(k\rho)\cos n\theta \\ &= \sum_{n=-\infty}^{\infty}\left[\frac{\pi}{2}Y_n(kR) - \left(\ln\frac{k}{2} + \gamma\right)J_n(kR)\right]J_n(k\rho)\cos n\theta, \\ &\quad R \geq \rho. \end{aligned} \tag{26}$$

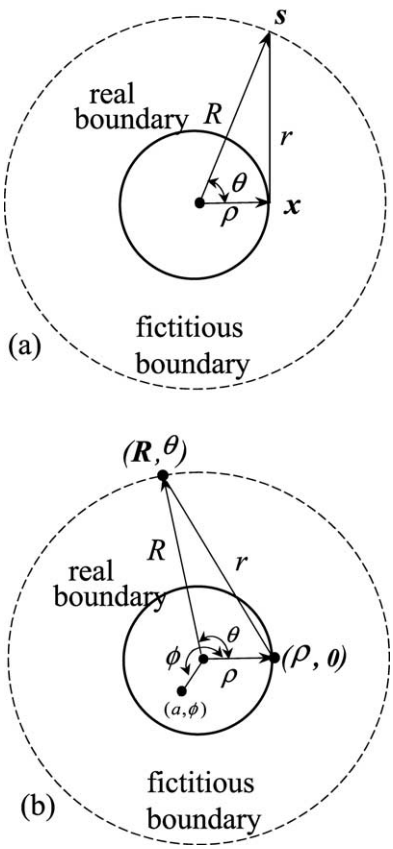

Fig. 1. (a) The definitions of ρ, θ, and R. (b) The definitions of a and ϕ.

It is interesting to find that the difference between the MRM kernel and real-part kernel stems from the loss terms of real constant, $ln(k/2)+\gamma$, in the zeroth-order fundamental solution [3].

The T kernel can be obtained by differentiating Eq. (26) with respect to ρ :

$$T(s,x)=\frac{\partial U}{\partial \rho}$$

$$=k\sum_{n=-\infty}^{\infty}\left[\frac{\pi}{2}Y_n(kR)-\left(\ln\frac{k}{2}+\gamma\right)J_n(kR)\right]J_n'(k\rho)\cos n\theta. \tag{27}$$

Based on the dual series representation for the kernels and Fourier expansion for $u(s)$ and $t(s)$ on the circular boundary, we have

$$t(s)=\sum_{n=1}^{N}(a_n\cos n\theta+b_n\sin n\theta)+a_0, \tag{28}$$

$$u(s)=\sum_{n=1}^{N}(c_n\cos n\theta+d_n\sin n\theta)+c_0. \tag{29}$$

The kernels can be expressed

$$U(s,x)=U(\phi-\theta)=\sum_{-\infty}^{\infty}S_m\cos m(\phi-\theta), \tag{30}$$

$$L(s,x)=L(\phi-\theta)=\sum_{-\infty}^{\infty}V_m\cos m(\phi-\theta), \tag{31}$$

where

$$S_m=\left[\frac{\pi}{2}Y_m(kR)-\left(\ln\frac{k}{2}+\gamma\right)J_m(kR)\right]J_m(k\rho), \tag{32}$$

$$V_m=k\left[\frac{\pi}{2}Y_m'(kR)-\left(\ln\frac{k}{2}+\gamma\right)J_m'(kR)\right]J_m(k\rho). \tag{33}$$

Substituting Eqs. (28)–(33) into the boundary integrals, we have

$$\begin{aligned}\int_B U(s,x)t(s)\mathrm{d}B(s)&=\int_0^{2\pi}U(s,x)t(s)R\mathrm{d}\theta\\&=\int_0^{2\pi}\left[a_0+\sum_{n=1}^{N}(a_n\cos n\theta+b_n\sin n\theta)\right]\\&\quad\times\sum_{m=-\infty}^{\infty}S_m\cos m(\theta-\phi)R\mathrm{d}\theta\\&=2\pi R\left[a_0S_0+\sum_{n=1}^{N}(a_n\cos n\phi+b_n\sin n\phi)S_n\right],\end{aligned} \tag{34}$$

$$\int_B L(s,x)t(s)\mathrm{d}B(s)$$

$$=2\pi R\left[a_0V_0+\sum_{n=1}^{N}(a_n\cos n\phi+b_n\sin n\phi)V_n\right], \tag{35}$$

where $x=(a,\phi)$ and ϕ are shown in Fig. 1(b). By setting the collocation points x with $\phi_m=m\Delta\theta$, $m=0,1,\ldots,2N$, and $\Delta\theta=\frac{2\pi}{2N+1}$, Eqs. (34) and (35) can be expressed as

$$(2\pi R)\begin{bmatrix}S_0 & S_1 & 0 & \cdots & S_N & 0\\ S_0 & S_1\cos\phi_1 & S_1\sin\phi_1 & \cdots & S_N\cos N\phi_1 & S_N\sin N\phi_1\\ S_0 & S_1\cos\phi_2 & S_1\sin\phi_2 & \cdots & S_N\cos N\phi_2 & S_N\sin N\phi_2\\ \vdots & \vdots & \vdots & & \vdots & \vdots\\ S_0 & S_1\cos\phi_{2N} & S_1\sin\phi_{2N} & \cdots & S_N\cos N\phi_{2N} & S_N\sin N\phi_{2N}\end{bmatrix}\begin{Bmatrix}a_0\\a_1\\b_1\\\vdots\\a_N\\b_N\end{Bmatrix}$$

$=2\pi R[B]\{a\}$ using single layer method or UT MRM method, (36)

and

$$(2\pi R)\begin{bmatrix} V_0 & V_1 & 0 & \cdots & V_N & 0 \\ V_0 & V_1\cos\phi_1 & V_1\sin\phi_1 & \cdots & V_N\cos N\phi_1 & V_N\sin N\phi_1 \\ V_0 & V_1\cos\phi_2 & V_1\sin\phi_2 & \cdots & V_N\cos N\phi_2 & V_N\sin N\phi_2 \\ \vdots & \vdots & \vdots & & \vdots & \vdots \\ V_0 & V_1\cos\phi_{2N} & V_1\sin\phi_{2N} & \cdots & V_N\cos N\phi_{2N} & V_N\sin N\phi_{2N} \end{bmatrix}\begin{Bmatrix} a_0 \\ a_1 \\ b_1 \\ \vdots \\ a_N \\ b_N \end{Bmatrix}$$

$$= 2\pi R[A]\{a\} \text{ using the double layer method or LM MRM method,} \tag{37}$$

where $\{a\}$ is a column vector of $(a_0,a_1,b_1,...,a_N,b_N)^{\mathrm{T}}$. It is easy to decompose $[B]$ and $[A]$ into

$$[B]=[H][D_B], \tag{38}$$

$$[A]=[H][D_A], \tag{39}$$

where

$$[H]=\begin{bmatrix} 1 & 1 & 0 & \cdots & 1 & 0 \\ 1 & \cos\phi_1 & \sin\phi_1 & \cdots & \cos N\phi_1 & \sin N\phi_1 \\ 1 & \cos\phi_2 & \sin\phi_2 & \cdots & \cos N\phi_2 & \sin N\phi_2 \\ \vdots & \vdots & \vdots & & \vdots & \vdots \\ 1 & \cos\phi_{2N} & \sin\phi_{2N} & \cdots & \cos N\phi_{2N} & \sin N\phi_{2N} \end{bmatrix}, \tag{40}$$

and

$$[D_B]=\begin{bmatrix} S_0 & & & & & \\ & S_1 & & & & \\ & & S_1 & & & \\ & & & \ddots & & \\ & & & & S_N & \\ & & & & & S_N \end{bmatrix}, \tag{41}$$

$$[D_A]=\begin{bmatrix} V_0 & & & & & \\ & V_1 & & & & \\ & & V_1 & & & \\ & & & \ddots & & \\ & & & & V_N & \\ & & & & & V_N \end{bmatrix}. \tag{42}$$

Using the following properties for $[H]$ (as shown in Appendix A)

$$[H]^{\mathrm{T}}[H]=\begin{bmatrix} 2N+1 & & & & & \\ & \frac{2N+1}{2} & & & 0 & \\ & & \frac{2N+1}{2} & & & \\ & & & \ddots & & \\ & 0 & & & \frac{2N+1}{2} & \\ & & & & & \frac{2N+1}{2} \end{bmatrix}, \tag{43}$$

we have

$$\det|[B]|=\det|H|\cdot\det|D_B|$$

$$=-2^{-N}[2N+1]^{N+(1/2)}\cdot S_0(S_1S_2...S_N)^2, \tag{44}$$

$$\det|[A]|=\det|H|\cdot\det|D_A|$$

$$=-2^{-N}[2N+1]^{N+(1/2)}\cdot V_0(V_1V_2...V_N)^2. \tag{45}$$

When $S_n=0$, $n=0,1,2,...,N$, true and spurious eigenvalues are imbedded in $[(\pi/2)Y_n(kR)-(\ln(k/2)+\gamma)J_n(kR)]J_n(k\rho)=0$ if the single layer potential method or UT method is used for the Dirichlet problem. We can summarize this as follows:

$$\text{True eigenequation}: \quad J_n(k\rho)=0 \tag{46}$$

for the Dirichlet problem;

$$\text{True eigenequation}: J_n'(k\rho)=0 \tag{47}$$

for the Neumann problem;

Spurious eigenequation :

$$\frac{\pi}{2}Y_n(kR)-\left(\ln\frac{k}{2}+\gamma\right)J_n(kR)=0 \quad \text{using MRM(UT).} \tag{48}$$

If the singularity is superimposed on the real boundary (ρ,θ), $0<\theta<2\pi$, instead of the fictitious boundary (R,θ), $0<\theta<2\pi$, then only the spurious eigenequation (48) is changed to

Spurious eigenequation :

$$\frac{\pi}{2}Y_n(k\rho)-\left(\ln\frac{k}{2}+\gamma\right)J_n(k\rho)=0 \quad \text{using MRM(UT).} \tag{49}$$

Both cases (true and spurious) have the same boundary modes, $e^{in\theta}$, on the boundary with radius R or ρ if UT MRM or single layer MRM is used.

If the LM formulation is used, we have

$$L=\frac{\partial U}{\partial R}=k\sum_{n=-\infty}^{\infty}\left[\frac{\pi}{2}Y_n'(kR)-\left(\ln\frac{k}{2}+\gamma\right)J_n'(kR)\right]J_n(k\rho)\times\cos n\theta, \tag{50}$$

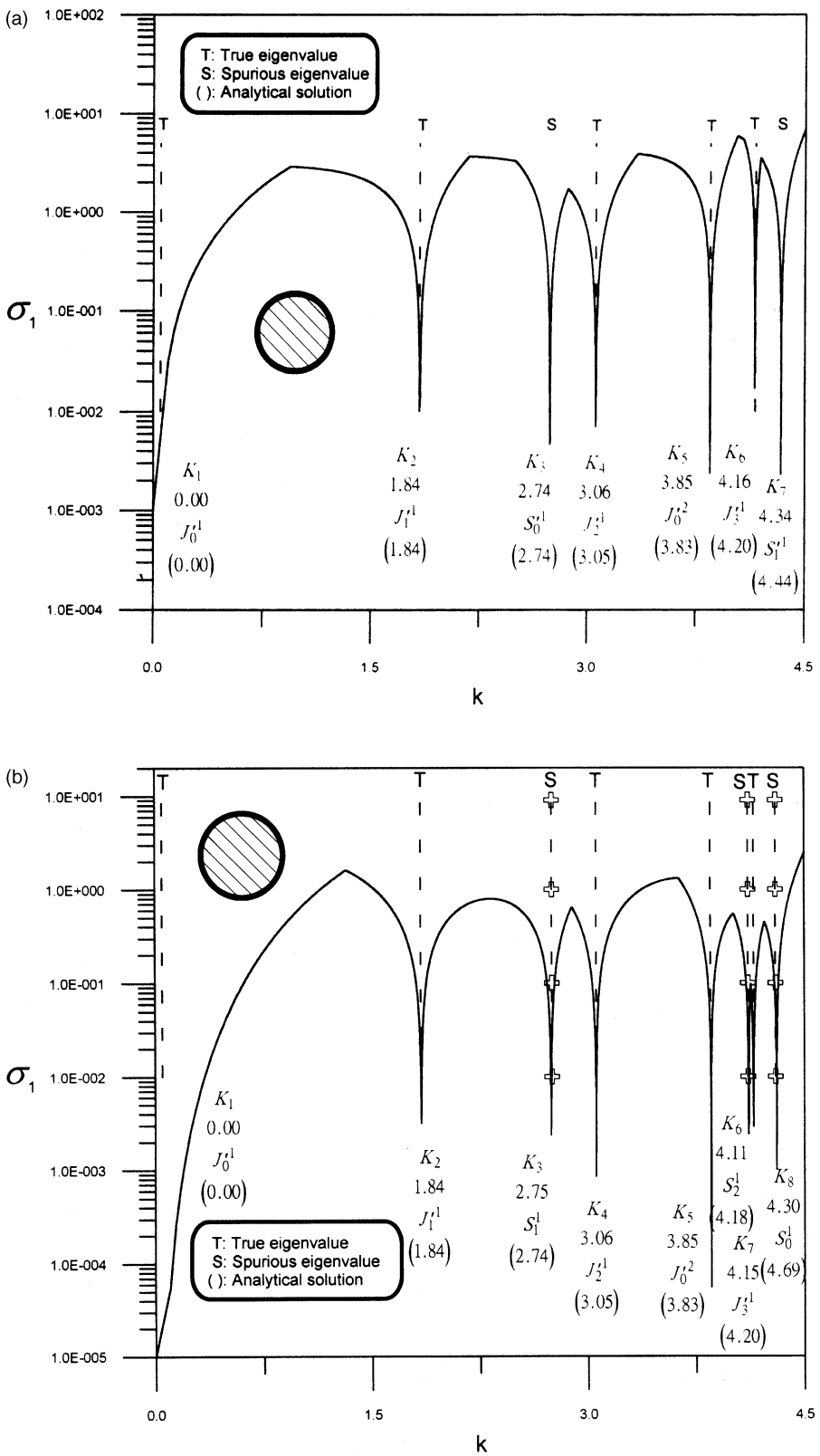

Fig. 2. (a) The minimum singular value σ_1 versus k using the UT equation only. (b) The minimum singular value σ_1 versus k using the LM equation only. (c) The minimum singular values σ_1 versus k results obtained using the UT and LM equations. (d) The second minimum singular value σ_2 versus k results obtained using the UT and LM equations. (e) The minimum singular value σ_1 versus k results obtained combining two equations from T matrix and all equations from M matrix. (f) The second minimum singular value σ_2 versus k results obtained combining two equations from T matrix and all equations from M matrix.

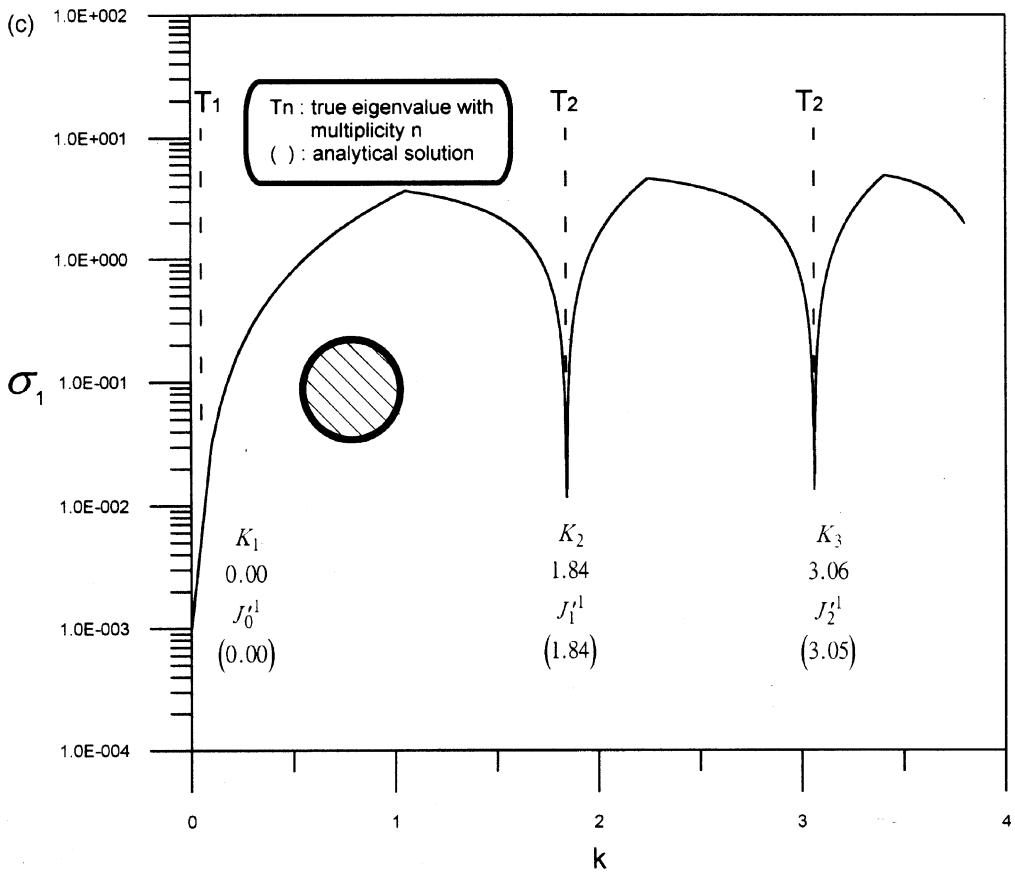

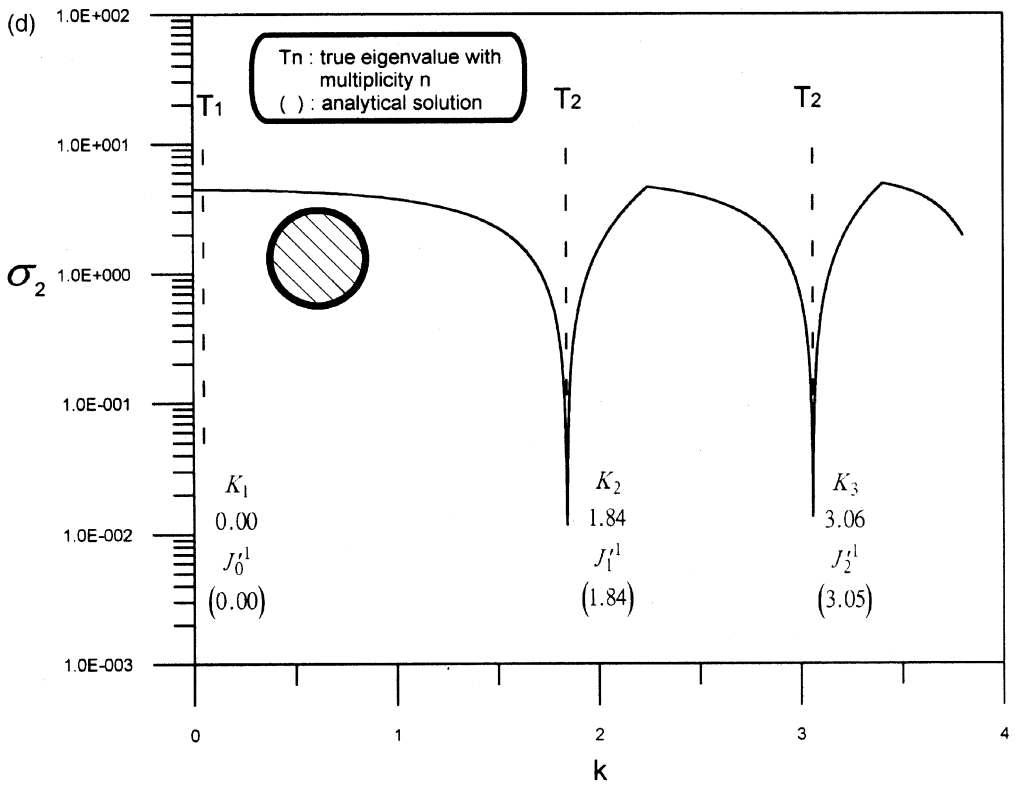

Fig. 2 (*continued*)

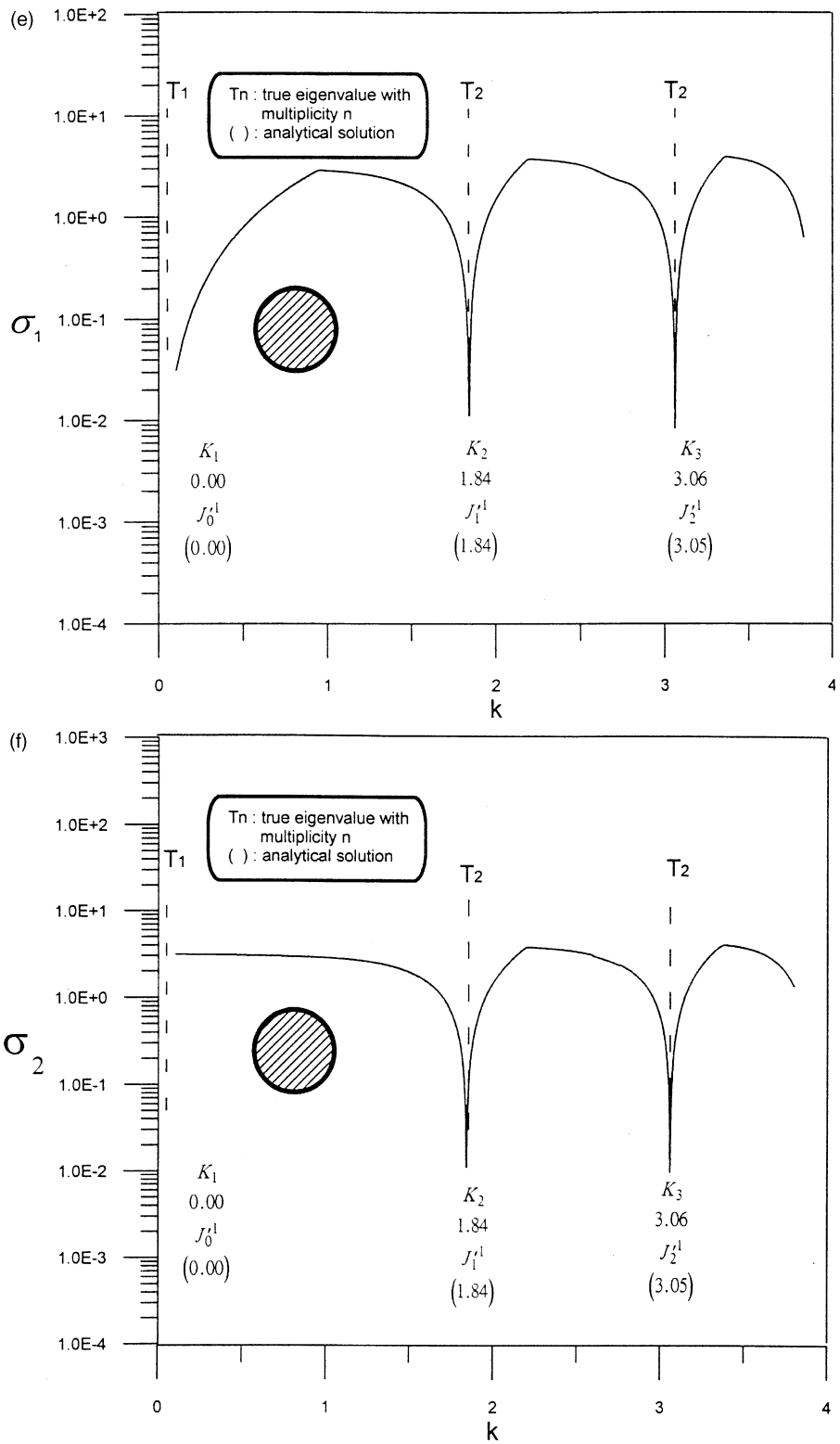

Fig. 2 (*continued*)

$$M = \frac{\partial^2 U}{\partial R \partial \rho} = k^2 \sum_{n=-\infty}^{\infty} \left[\frac{\pi}{2} Y_n'(kR) - \left(\ln \frac{k}{2} + \gamma \right) J_n'(kR) \right] \times J_n'(k\rho) \cos n\theta. \tag{51}$$

Similarly, the true and spurious eigenvalues occur at the zeros for the following spurious eigenequation:

True eigenequation :

$$J_n(k\rho) = 0 \text{ for Dirichlet problem;} \tag{52}$$

True eigenequation :

$$J'_n(k\rho) = 0 \text{ for the Neumann problem;} \tag{53}$$

Spurious eigenequation :

$$\frac{\pi}{2} Y'_n(kR) - \left(\ln\frac{k}{2} + \gamma\right) J'_n(kR) = 0 \tag{54}$$

using fictitious MRM(LM);

Spurious eigenequation :

$$\frac{\pi}{2} Y'_n(k\rho) - \left(\ln\frac{k}{2} + \gamma\right) J'_n(k\rho) \tag{55}$$

$= 0$ using direct MRM(LM).

Both cases (true and spurious) have the same boundary modes, $e^{in\theta}$, on the boundary with radius R or ρ if LM MRM or double layer MRM is used.

Substituting the eigenvalues and boundary modes (obtained from the MRM UT equation) into UT equation (1) for an interior point, we have

$$u_n(a,\phi) = \pi^2 R J_n(ka)\left[\frac{\pi}{2} Y_n(k\rho) - \left(\ln\frac{k}{2} + \gamma\right) J_n(k_\rho)\right] \times (\alpha\cos(n\phi) + \beta\sin(n\phi)), \tag{56}$$

$0 < a < \rho,\ \ 0 < \phi < 2\pi,$

where α and β are free constants. Similarly, we have

$$u_n(a,\phi) = \pi^2 R J_n(ka)\left[\frac{\pi}{2} Y'_n(k\rho) - \left(\ln\frac{k}{2} + \gamma\right) J'_n(k_\rho)\right] \times (\alpha\cos(n\phi) + \beta\sin(n\phi)), \tag{57}$$

$0 < a < \rho,\ \ 0 < \phi < 2\pi,$

if the MRM LM equation is used. Theoretically, it is interesting to find that spurious modes are trivial since the terms of $[(\pi/2)Y_n(k\rho) - (\ln(k/2) + \gamma)J_n(k\rho)]$ and $[(\pi/2)Y'_n(k\rho) - (\ln(k/2) + \gamma)J'_n(k\rho)]$ are imbedded in Eqs. (56) and (57), respectively. However, the spurious modes obtained numerically are as follows using UT MRM and LM MRM, respectively, where $\bar{u}_n(a,\phi)$ is a normalized mode:

Single layer or UT method :

$$\bar{u}_n(a,\phi) = J_n(ka)(\alpha\cos(n\phi) + \beta\sin(n\phi)), \tag{58}$$

$0 < a < \rho,\ \ 0 < \phi < 2\pi;$

Double layer or LM method :

$$\bar{u}_n(a,\phi) = J_n(ka)(\alpha\cos(n\phi) + \beta\sin(n\phi)), \tag{59}$$

$0 < a < \rho,\ \ 0 < \phi < 2\pi.$

It is interesting to find that the nodal lines for true and spurious modes are the same after normalization if $[(\pi/2)Y_n(k\rho) - (\ln(k/2) + \gamma)J_n(k\rho)]$ or $[(\pi/2)Y'_n(k\rho) - (\ln(k/2) + \gamma)J'_n(k\rho)]$ approaches zero but is not exactly zero. To be precise, true and spurious modes are different since eigenvalues are not equal.

6. Numerical examples—a circular cavity and a square cavity

In the first case of circular cavity with radius 1, an analytical solution is available as follows: eigenequation $J'_m(k_{mn}\rho) = 0,\ \ m = 0,1,2,3,\ldots;\ \ n = 1,2,3,\ldots;$ eigenmode: $u(a,\theta) = J_m(k_{mn}a)e^{im\theta},\ 0 < a < \rho,\ 0 < \theta < 2\pi$.

Eighty elements for $\rho = 1$ are adopted in the boundary element mesh. Since two alternatives, the UT and LM equation, can be chosen when collocating on the boundary, two results from the UT and LM methods can be obtained. Fig. 2(a) shows the minimum singular value versus k. The true eigenvalues contaminated by spurious eigenvalues can be obtained as shown in Fig. 2(a) by considering the near zero minimum singular values if only the UT equation is chosen. In a similar way, the true eigenvalues contaminated by spurious eigenvalues can be obtained as shown in Fig. 2(b) by considering the near zero minimum singular values if only the LM equation is chosen. It is interesting to find that no spurious eigenvalues occur as shown in Fig. 2(c) when the UT and LM equations are combined. After obtaining the true eigenvalues, their multiplicities can be determined as shown in Fig. 2(d) from the locations where the second minimum singular value also approaches zero. It is found that double roots are obtained in this case. Since no triple roots are available, the plot of σ_3 versus k is not provided. The true and spurious eigenvalues are shown in Tables 1 and 2, respectively. The ABAQUS results in Refs. [25,26] for the true eigensolutions also match the present solutions. Good agreement between analytical and numerical results can be obtained. For the more efficient method, two equations from T matrix are combined with all

Table 1
The true eigenvalues obtained by using the analytical method and MRM for a circular domain with Neumann boundary conditions

	1	2	3	4
Analytical solution	1.8412 (J'^1_1)	3.0542 (J'^1_2)	3.8317 (J'^2_0)	4.2012 (J'^1_3)
Numerical solution using UT equation (MRM)	1.84	3.06	3.85	4.15
Numerical solution using LM equation (MRM)	1.84	3.06	3.85	4.16

$J'_m n$ denotes the eigenvalues which satisfy the true eigenequation: $J'_m(k_{mn}\rho) = 0,\ m = 0,1,2,3,\ldots,\ n = 1,2,3,\ldots$

Table 2
The spurious eigenvalues obtained by using the analytical method and MRM for a circular domain with Neumann boundary conditions

	1	2
Analytical spurious eigenvalues using UT equation (MRM)	2.74 (S_1^1)	4.18 (S_2^1)
Numerical spurious eigenvalues using UT equation (MRM)	2.75	4.11
Analytical spurious eigenvalues using LM equation (MRM)	2.74 ($S_0'1$)	4.44 ($S_1'1$)
Numerical spurious eigenvalues using UT equation (MRM)	2.74	4.34

S_m^n denotes the eigenvalues which satisfy the spurious eigenequation: $(\pi/2)Y_m(k_{mn}\rho) - (\ln(k_{mn}/2) + \gamma)J_m(k_{mn}\rho) = 0$, $m = 0, 1, 2, \ldots$, $n = 1, 2, \ldots$ by MRM (UT). $S_m^{'n}$ denotes the eigenvalues which satisfy the spurious eigenequation: $(\pi/2)Y_n'(k_{mn}\rho) - (\ln(k_{mn}/2) + \gamma)J_m'(k_{mn}\rho) = 0$, $m = 0, 1, 2, \ldots$, $n = 1, 2, \ldots$ by MRM (LM).

the equations from M matrix and the results are shown in Fig. 2(e) and (f). Good agreement can be made in comparison with Fig. 2(c) and (d). In Fig. 2, there are sharp changes in the slopes of curve. This is a natural result instead of artificial plot. Since the function of $\sigma_1(k)$, is the minimum of all the singular values of function k, $(\sigma_1(k), \sigma_2(k), \sigma_3(k), \ldots,)$, the abrupt change of slopes can be understood as an envelope curve. The first four true boundary and interior modes are shown in Figs. 3 and 4, respectively. The first two spurious boundary and interior modes are shown in Figs. 5 and 6, respectively. Some contamination near the boundary can be found in the interior modes. The analytical and numerical results match very well. As expected, the spurious modes in Figs. 5 and 6 for Eqs. (56) and (57) are found to have the same nodal lines that the true modes have although they have different eigenvalues. Table 3 summarizes the results for the Neumann problem. Also, the true and spurious eigensolutions for the Dirichlet problem can be derived analytically as

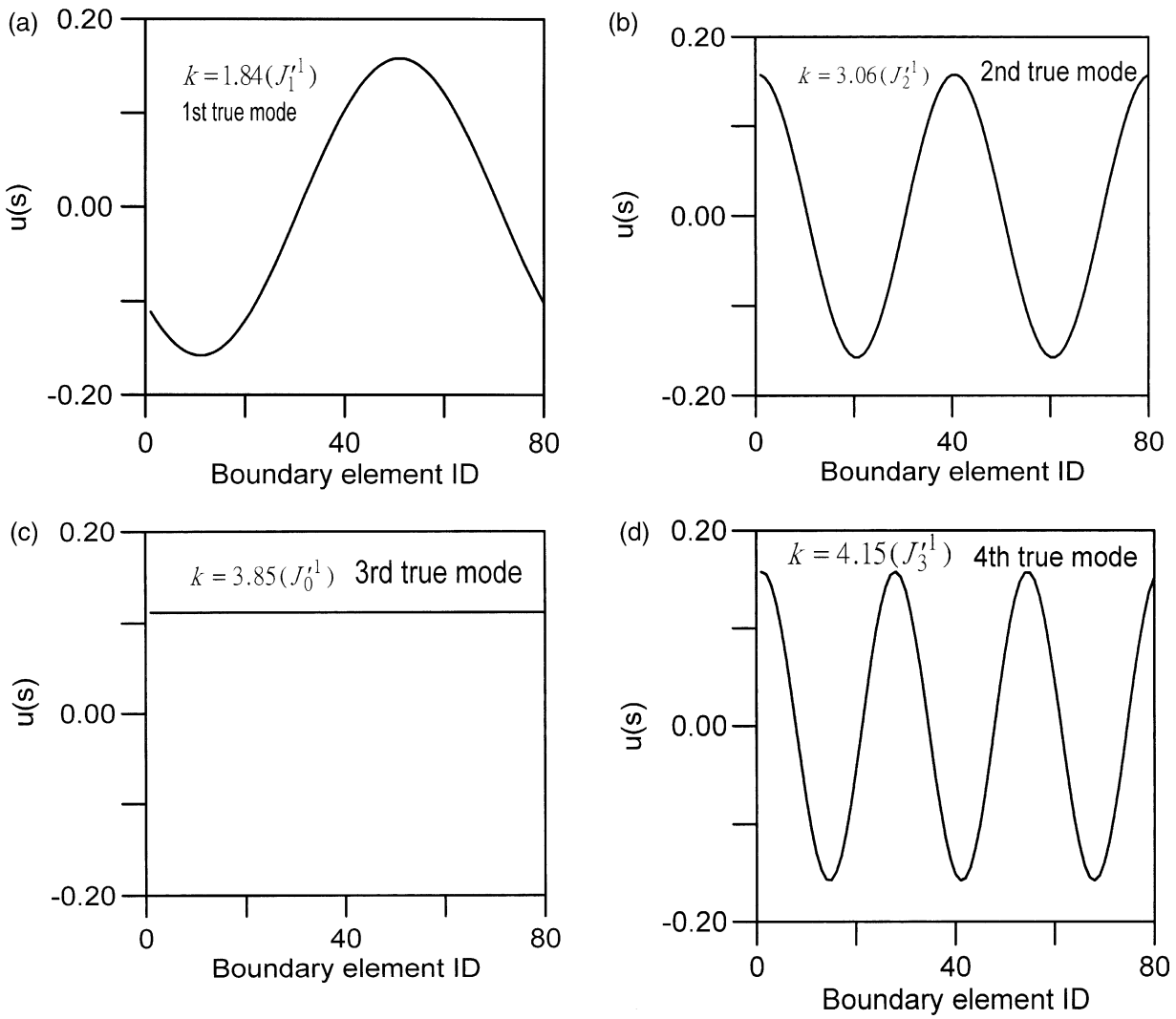

Fig. 3. (a) The first true boundary modes. (b) The second true boundary modes. (c) The third true boundary modes. (d). The fourth true boundary modes.

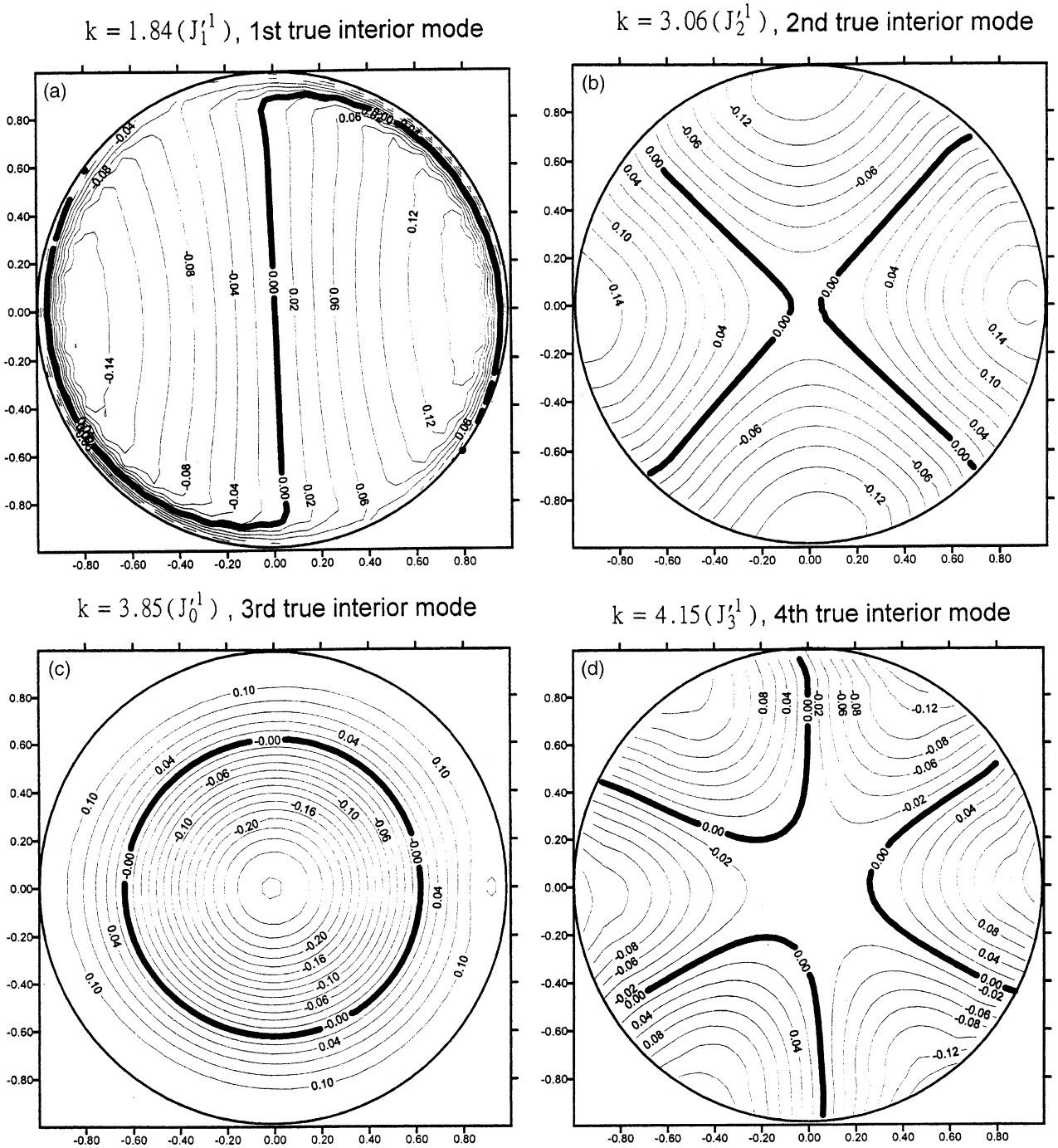

Fig. 4. (a) The first true interior modes. (b) The second true interior modes. (c) The third true interior modes. (d) The fourth true interior modes.

shown in Table 4. Although the spurious eigen solution of a noncircular case cannot be analytically predicted, the numerical results are shown in Fig. 7(a)–(e). The results agree well with the exact solution of true eigensolution. Since the CPU time of the MRM depends on the number of adopted terms, the comparison with the other methods is not provided.

7. Conclusions

The dual MRM in conjunction with the SVD technique has been applied to determine the eigensolutions of a circular cavity. Analytical solutions for the true and spurious eigensystems occuring in the UT or LM equation only have been derived. A more efficient method has been

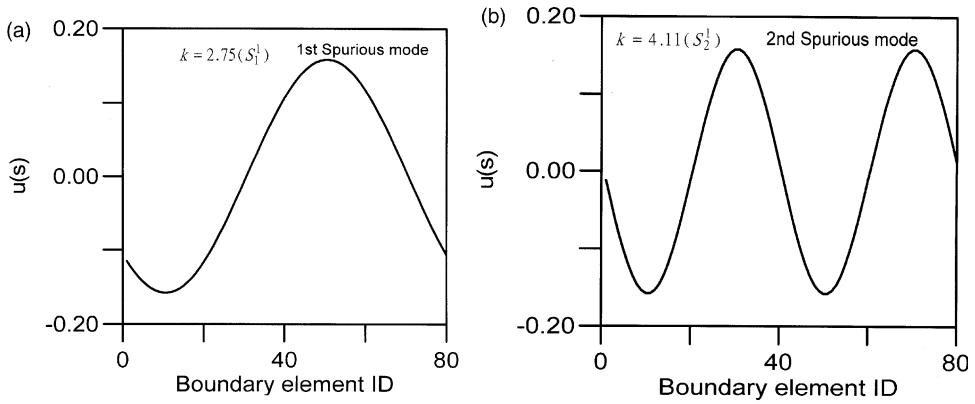

Fig. 5. (a) The first spurious boundary modes. (b) The second spurious boundary modes.

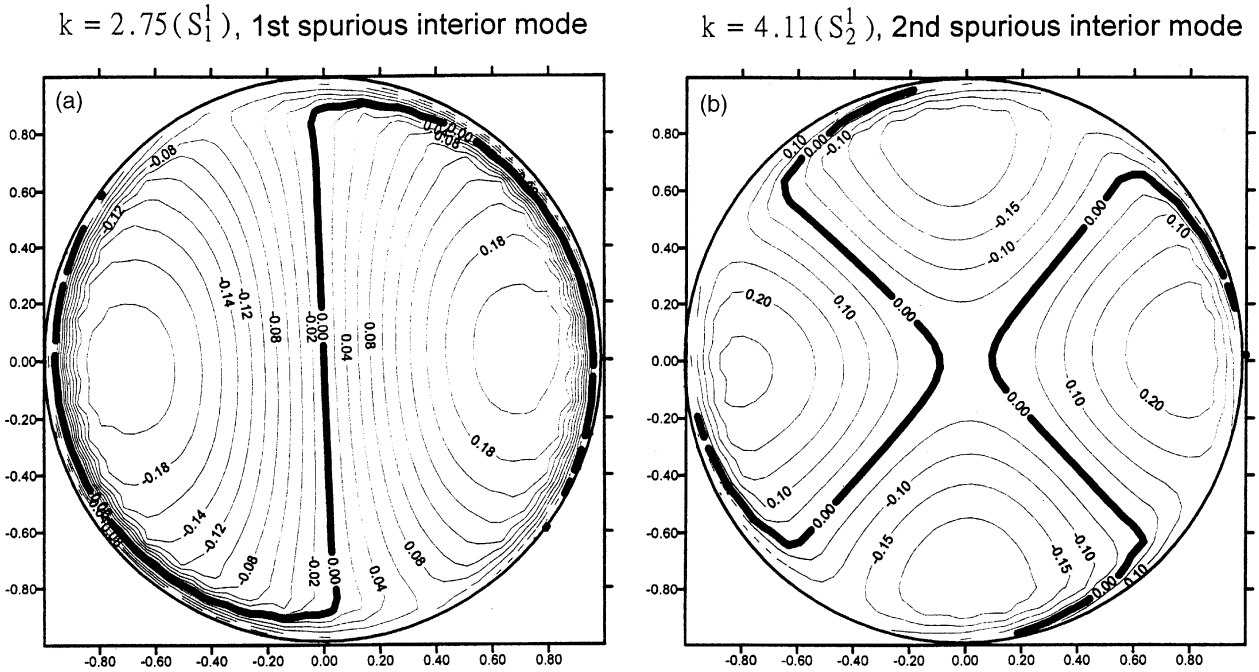

Fig. 6. (a) The first spurious interior modes. (b) The second spurious interior modes.

Table 3
The true and spurious systems for the Neumann problem using UT MRM and LM MRM

	Eigenequation		Eigenmode (boundary)	Eigenmode (interior): $u_n(a,\phi)$: (unnormalized); Eigenmode (interior): $\bar{u}_n(a,\phi)$: (normalized)
UT method	True	$J_n'(k\rho)=0$	$e^{in\theta}$	$u_n(a,\phi)=\pi^2 RJ_n(ka)[\frac{\pi}{2}Y_n(k\rho)-(\ln\frac{k}{2}+\gamma)J_n(k\rho)]\cos(n\phi)$[a] $\bar{u}_n(a,\phi)=J_n(ka)\cos(n\phi)$[b]
	Spurious	$\frac{\pi}{2}Y_n(k\rho)-(\ln\frac{k}{2}+\gamma)J_n(k\rho)=0$	$e^{in\theta}$	$u_n(a,\phi)=\pi^2 RJ_n(ka)[\frac{\pi}{2}Y_n(k\rho)-(\ln\frac{k}{2}+\gamma)J_n(k\rho)]\cos(n\phi)$[c] $\bar{u}_n(a,\phi)=J_n(ka)\cos(n\phi)$[b]
LM method	True	$J_n'(k\rho)=0$	$e^{in\theta}$	$u_n(a,\phi)=\pi^2 RJ_n(ka)[\frac{\pi}{2}Y_n'(k\rho)-(\ln\frac{k}{2}+\gamma)J_n'(k\rho)]\cos(n\phi)$[a] $\bar{u}_n(a,\phi)=J_n(ka)\cos(n\phi)$[b]
	Spurious	$\frac{\pi}{2}Y_n'(k\rho)-(\ln\frac{k}{2}+\gamma)J_n'(k\rho)=0$	$e^{in\theta}$	$u_n(a,\phi)=\pi^2 RJ_n(ka)[\frac{\pi}{2}Y_n'(k\rho)-(\ln\frac{k}{2}+\gamma)J_n'(k\rho)]\cos(n\phi)$[c] $\bar{u}_n(a,\phi)=J_n(ka)\cos(n\phi)$[b]

[a] Denotes a nontrivial solution.
[b] Denotes a nontrivial solution after normalization.
[c] Denotes a trivial solution without normalization.

Table 4
The true and spurious systems for the Dirichlet problem using UT MRM and LM MRM

	Eigenequation		Eigenmode (boundary)	Eigenmode (interior): $u_n(a,\phi)$: (unnormalized); eigenmode (interior): $\bar{u}_n(a,\phi)$ (normalized)
UT method	True	$J_n(k\rho)=0$	$e^{in\theta}$	$u_n(a,\phi)=\pi^2 RJ_n(ka)[\frac{\pi}{2}Y_n(k\rho)-(\ln\frac{k}{2}+\gamma)J_n(k\rho)]\cos(n\phi)$[a] $\bar{u}_n(a,\phi)=J_n(ka)\cos(n\phi)$[b]
	Spurious	$\frac{\pi}{2}Y_n(k\rho)-(\ln\frac{k}{2}+\gamma)J_n(k\rho)=0$	$e^{in\theta}$	$u_n(a,\phi)=\pi^2 RJ_n(ka)[\frac{\pi}{2}Y_n(k\rho)-(\ln\frac{k}{2}+\gamma)J_n(k\rho)]\cos(n\phi)$[c] $\bar{u}_n(a,\phi)=J_n(ka)\cos(n\phi)$[b]
LM method	True	$J_n(k\rho)=0$	$e^{in\theta}$	$u_n(a,\phi)=\pi^2 RJ_n(ka)[\frac{\pi}{2}Y'_n(k\rho)-(\ln\frac{k}{2}+\gamma)J'_n(k\rho)]\cos(n\phi)$[a] $\bar{u}_n(a,\phi)=J_n(ka)\cos(n\phi)$[b]
	Spurious	$\frac{\pi}{2}Y'_n(k\rho)-(\ln\frac{k}{2}+\gamma)J'_n(k\rho)=0$	$e^{in\theta}$	$u_n(a,\phi)=\pi^2 RJ_n(ka)[\frac{\pi}{2}Y'_n(k\rho)-(\ln\frac{k}{2}+\gamma)J'_n(k\rho)]\cos(n\phi)$[c] $\bar{u}_n(a,\phi)=J_n(ka)\cos(n\phi)$[b]

[a] Denotes a nontrivial solution.
[b] Denotes a nontrivial solution after normalization.
[c] Denotes a trivial solution without normalization.

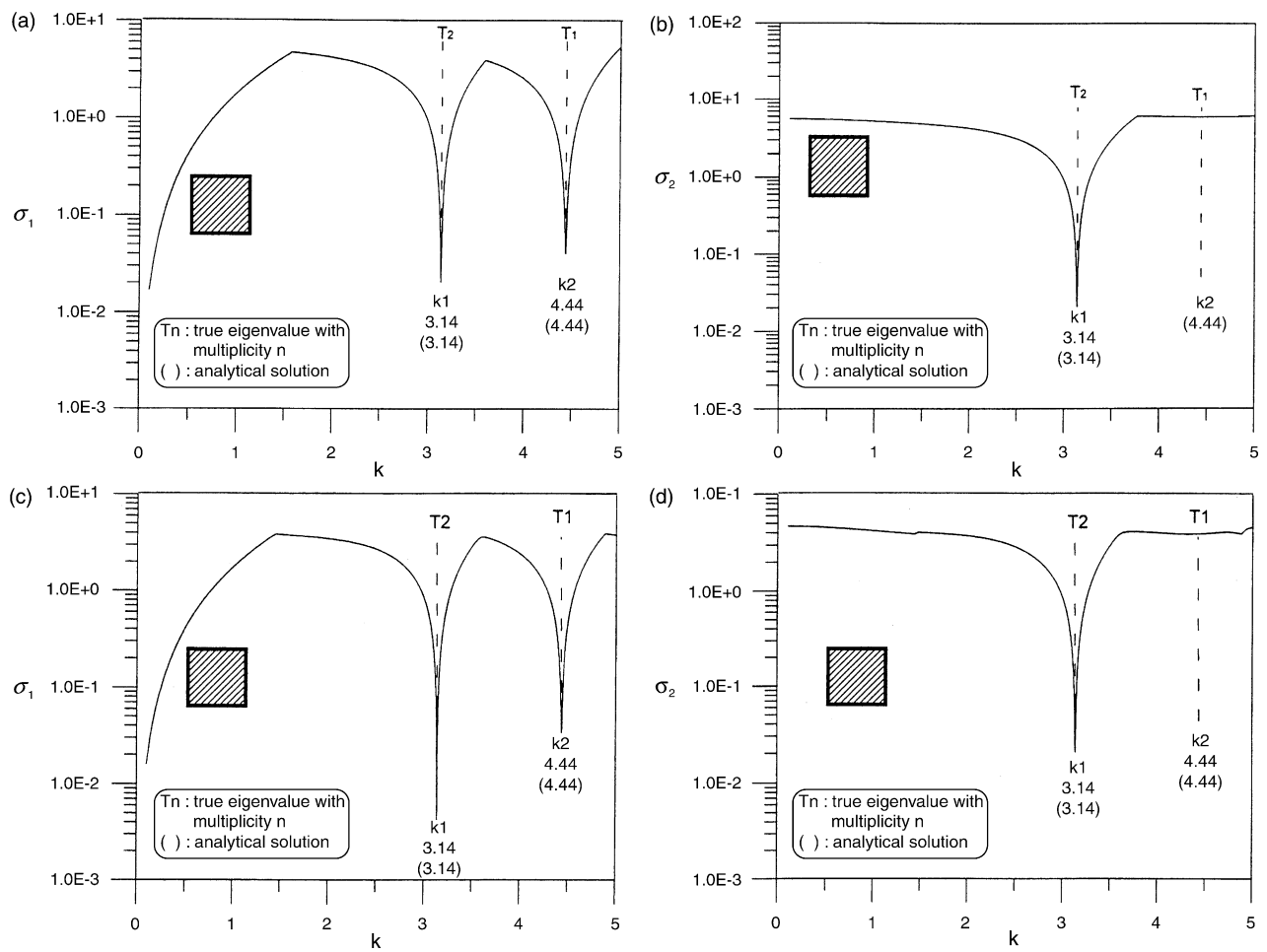

Fig. 7. (a) The minimum singular value σ_1 versus k results obtained using the UT and LM equations only. (b) The second minimum singular value σ_2 versus k results obtained using the UT and LM equations. (c) The minimum singular value σ_1 versus k results obtained combining two equations from T matrix and all equations from M matrix. (d) The second minimum singular value σ_2 versus k results obtained combining two equations from T matrix and all equations from M matrix.

proposed by selecting sufficient number of equations from dual MRM instead of all of them. Numerical experiments have been performed to filter out the spurious solutions by using the dual formulation. A general purpose program, DUALMRM, has been developed, the spurious solutions have been successfully predicted analytically and filtered out numerically, and the multiplicities and boundary modes of the true solutions for the circular cavities have been

determined by using the SVD technique. The possible application of MRM to large scale problem will be conducted in the future work.

Acknowledgements

Financial support from the National Science Council under Grant No. NSC-88-2211-E-019-005 for National Taiwan Ocean University is gratefully acknowledged.

Appendix A

Using the property of a geometric series, we have

$$\sum_{n=0}^{2N} e^{in\phi_m} = \frac{1 - e^{i(2N+1)\phi_m}}{1 - e^{i\phi_m}}, \tag{A1}$$

$$\sum_{n=0}^{2N} e^{in\phi_m} = \frac{1 - e^{im2\pi}}{1 - e^{i\phi_m}} = 0 \qquad (m \neq 0), \tag{A2}$$

where

$$\phi_m = m\,\Delta\theta = \frac{2m\pi}{2N+1}.$$

Also, we have

$$\sum_{n=0}^{2n} \cos n\phi_m = \begin{cases} 0, & (m \neq 0), \\ 2N+1, & (m = 0), \end{cases} \tag{A3}$$

$$\sum_{n=0}^{2n} \sin n\phi_m = 0 \qquad (m = 0, 1, 2, \ldots, 2N), \tag{A4}$$

$$\sum_{n=0}^{2N} \cos \mu\phi_n \sin \lambda\phi_n = \sum_{n=0}^{2N} \cos n\mu\phi_1 \sin n\lambda\phi_1$$

$$(\phi_n = n\,\Delta\theta = n\phi_1) \tag{A5}$$

$$= \tfrac{1}{2} \sum_{n=0}^{2N} [\sin n(\lambda + \mu)\phi_1 + \sin n(\lambda - \mu)\phi_1] = 0,$$

$$\sum_{n=0}^{2N} \sin \mu\phi_n \sin \lambda\phi_n$$

$$= \tfrac{1}{2} \sum_{n=0}^{2N} [\cos n(\lambda - \mu)\phi_1 - \cos n(\lambda + \mu)\phi_1]$$

$$= \begin{cases} 0, & \lambda \neq \mu, \\ \dfrac{1}{2}(2N+1), & \lambda = \mu, \end{cases}, \tag{A6}$$

$$\sum_{n=0}^{2N} \sin \mu\phi_n \cos \lambda\phi_n$$

$$= \frac{1}{2} \sum_{n=0}^{2N} [\cos n(\lambda - \mu)\phi_1 + \cos n(\lambda + \mu)\phi_1]$$

$$= \begin{cases} 0, & \lambda \neq \mu, \\ \dfrac{1}{2}(2N+1), & \lambda = \mu \neq 0, \\ 2N+1, & \lambda = \mu = 0, \end{cases} \tag{A7}$$

where

$$\lambda = 0, 1, 2, \ldots, N$$

$$\mu = 0, 1, 2, \ldots, N.$$

References

[1] Nowak AJ, Neves AC, editors. Multiple reciprocity boundary element method. Southampton: Computational Mechanics Publications; 1994.

[2] Kamiya N, Andoh E, Nogae K. A new complex-valued formulation and eigenvalue analysis of the Helmholtz equation by boundary element method. Adv Engng Software 1996;26: 219–27.

[3] Chen JT. In: Onate E, Idelsohn SR, editors. Recent development of dual BEM in acoustic problems, keynote lecture. Proceedings of the Fourth World Congress on Computational Mechanics, Argentina; 1998. p. 106.

[4] Chen JT, Huang CS, Wong FC. Analysis and experiment for acoustic modes of a cavity containing an incomplete partition. Proc Fourth Nat Conf Struct Engng 1998;1:349–56.

[5] De Mey. Calculation of the Helmholtz equation by an integral equation. Int J Numer Meth Engng 1976;10:59–66.

[6] De Mey. A simplified integral equation method for the calculation of the eigenvalues of the Helmholtz equation. Int J Numer Meth Engng 1977;11:1340–2.

[7] Chang JR, Yeih W, Chen JT. Determination of natural frequencies and natural modes using the dual BEM in conjunction with the domain partition technique. Comput Mech 1999;24(1):29–40.

[8] Chen JT, Wong FC. Analytical derivations for one-dimensional eigenproblems using dual BEM and MRM. Engng Anal Bound Elem 1997;20(1):25–33.

[9] Chen JT, Huang CX, Chen KH. Determination of spurious eigenvalues and multiplicities of true eigenvalues using the real-part dual BEM. Comput Mech 1999;24(1):41–51.

[10] Chen JT, Huang CX, Wong FC. Determination of spurious eigenvalues and multiplicities of true eigenvalues in the dual multiple reciprocity method using the singular value decomposition technique. J Sound Vib 2000;230(2):219–30.

[11] Kuo SR, Chen JT, Huang CX. Analytical study and numerical experiments for true and spurious eigensolutions of a circular cavity using the real-part dual BEM. J Numer Meth Engng 2000;48: 1401–22.

[12] Chen JT, Hong H-K. Review of dual integral representations with emphasis on hypersingular integrals and divergent series. Trans ASME, Appl Mech Rev 1999;52(1):17–33.

[13] Chen JT, Hong H-K. Boundary element method, 2nd ed. Taipei, Taiwan: New World Press; 1992. in Chinese.

[14] Burton AJ, Miller GF. The application of integral equation methods to the numerical solution of some exterior boundary-value problem. Proc R Soc Lond A 1971;323:201–10.

[15] Yeih W, Chen JT, Chen KH, Wong FC. A study on the multiple reciprocity method and complex-valued formulation for the Helmholtz equation. Adv Engng Software 1997;29(1): 7–12.
[16] Chen KH, Chen JT, Liou DY. Dual boundary element analysis for an acoustic cavity with an incomplete partition. Chin J Mech 1998;14(2): 1–11. in Chinese.
[17] Chen JT, Wong FC. Dual formulation of multiple reciprocity method for the acoustic mode of a cavity with a thin partition. J Sound Vib 1998;217(1):75–95.
[18] Yeih W, Chang JR, Chang CM, Chen JT. Applications of dual MRM for determining the natural frequencies and natural modes of a rod using the singular value decomposition method. Adv Engng Software 1999;30(7):459–68.
[19] Yeih W, Chen JT, Chang CM. Applications of dual MRM for determining the natural frequencies and natural modes of an Euler–Bernoulli beam using the singular value decomposition method. Engng Anal Bound Elem 1999;23(4):339–60.
[20] Chen JT, Chen KH, Chyuan SW. Numerical experiments for acoustic modes of a square cavity using dual BEM. Appl Acoust 1999;57(4): 293–325.
[21] Gloub GH, Van Loan CF. Matrix computations, 2nd edn. Baltimore: The Johns Hopkins University Press; 1989.
[22] Press WT, Teukosky SA, Vetterling WT, Flannery BP. Numerical recipes in FORTRAN, 2nd ed. New York: Cambridge University Press; 1992.
[23] Chen JT, Chen KH. Dual integral formulation for determining the acoustic modes of a two-dimensional cavity with a degenerate boundary. Engng Anal Bound Elem 1998;21(2):105–16.
[24] Liou DY, Chen JT, Chen KH. A new method for determining the acoustic modes of a two-dimensional sound field. J Chin Inst Civil Hydraul Engng 1999;11(2):299–310. in Chinese.
[25] Chen JT, Liang MT, Chen IL, Chyuan SW, Chen KH. Dual boundary element analysis of wave scattering from singularities. Wave Motion 1999;30(4):367–81.
[26] MSC/ABAQUS User Manual. MSC Version 5.5; 1996